Geophysical Research Letters

Maximum Southwest Greenland Ice Sheet Recession in the Early Holocene

A. J. Lesnek[1], J. P. Briner[2], N. E. Young[3], and J. K. Cuzzone[4]

[1]Department of Earth Sciences, University of New Hampshire, Durham, NH, USA, [2]Department of Geology, University at Buffalo, Buffalo, NY, USA, [3]Lamont-Doherty Earth Observatory, Columbia University, Palisades, NY, USA, [4]NASA Jet Propulsion Laboratory, California Institute of Technology, Pasadena, CA, USA

Abstract Establishing the timing of maximum Holocene warmth in the Arctic is critical for understanding global climate system response to external forcing. In Greenland, challenges in obtaining climate records that span the full Holocene have hampered efforts to robustly identify when the Holocene Thermal Maximum occurred. Reconstructing land-based ice sheet history can fill this gap because these ice sheet regions respond sensitively to summer temperature. We synthesize new and published ^{10}Be and ^{14}C ages from southwest Greenland to map Greenland ice sheet margin positions from 12 to 7 ka and calculate retreat rates from 12 to 0 ka. We found that maximum Greenland ice sheet recession occurred between ~10.4 and 9.1 ka. Our reconstruction suggests that summer air temperatures in southwest Greenland were highest from ~10.4 to 9.1 ka, providing support for an early regional Holocene Thermal Maximum. These results can serve as benchmarks for comparison with ice sheet and climate model simulations.

Plain Language Summary As the climate warms, Arctic temperatures are expected to increase at a faster rate than the rest of the world. Previous research has determined that Arctic temperatures were several degrees Celsius higher than today at some point in the past 12,000 years, and understanding when this warm time occurred might give scientists important insights into Arctic climate conditions in the future. However, in Greenland, the timing of maximum warmth is not well defined because many existing climate reconstructions do not span all of the past 12,000 years. In this paper, we use the retreat rate of the western Greenland ice sheet to determine when the warmest time of the past 12,000 years occurred. This method is advantageous because (1) retreat rates of this part of the Greenland ice sheet are directly related to summer air temperature and (2) the retreat history of the western Greenland ice sheet retreat is well known. We bring together new and previously published data that relates to Greenland ice sheet change to calculate how quickly the ice sheet retreated between 12,000 years ago and the present. Using this information, we determined that the warmest time of the past 12,000 years occurred between about 10,400 and 9,100 years ago, which is several thousand years earlier than some previous estimates. These results can help improve computer simulations that are used to predict future changes in Arctic ice sheet extent, climate, and sea-level.

1. Introduction

Understanding the pattern and timing of Arctic system response to past warmth can inform model-based predictions of cryosphere evolution under projected climate scenarios. Across the Arctic, a relative wealth of paleoclimate data exists for the Holocene, and proxy compilations suggest that both the onset (Briner et al., 2016; Kaufman et al., 2004) and the cessation (McKay et al., 2018) of the Holocene Thermal Maximum (HTM) varied spatially. However, in most of the Baffin Bay region (encompassing eastern Arctic Canada and western Greenland), the presence of the Greenland and Laurentide ice sheets prevented the deposition of terrestrial paleoclimate archives (e.g., lake sediments) for much of the early Holocene. Lacustrine records that do exist from Baffin Bay present conflicting evidence of the timing of maximum Holocene warmth, with some proxies suggesting temperatures were highest in the early Holocene (Axford et al., 2013), while others suggest the warmest interval occurred during the middle Holocene (Gajewski, 2015). Ice cores provide continuous records of Holocene climate, but uncertainties in ice surface elevation change through time can complicate climatic interpretations (Vinther et al., 2009). Similarly, climatic signals from marine sediment records can be obscured by ice sheet meltwater discharge (Lloyd et al., 2005). To
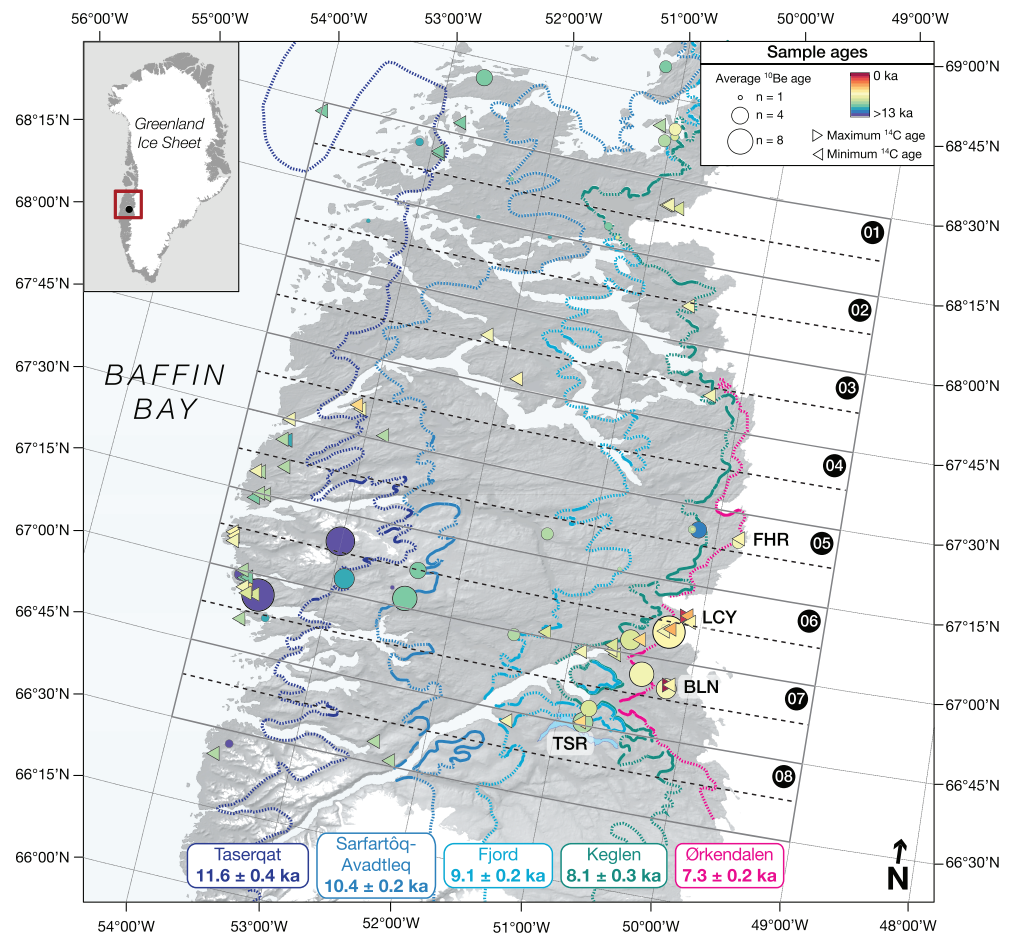
Figure 1. The Kangerlussuaq region. Early Holocene GrIS limits are indicated by the colored lines; mappable moraine crests are solid lines and interpolated ice margin positions are dotted lines. Moraine ages are shown as averages with 1 standard deviation (SD) external uncertainty. Chronologies used to draw GrIS limits are color-coded by age, ranging from >13 (purple) to 0 ka (red). Average ^{10}Be deglaciation ages are indicated by circles whose size correlates to the number of samples at a given location. Maximum-limiting ^{14}C ages are shown by right-facing triangles. Minimum-limiting ^{14}C ages are shown by left-facing triangles. Sources for previously published ^{14}C and ^{10}Be ages are listed in Tables S1 and S2, respectively. Locations of proglacial threshold lakes are indicated by three letter codes: FHR = Four Hare Lake, LCY = Lake Lucy, BLN = Baby Loon Lake, TSR = Tasersuaq. Gray rectangles indicate zones used to calculate area-integrated retreat rates. Zone numbers referenced in Table S4 are shown by the black circles. Profile lines used to calculate linear retreat rates and create swath topography for each zone are indicated by the dotted black lines. On the inset map, the black dot shows the location of the town of Kangerlussuaq.

firmly establish when the HTM occurred in the Baffin Bay region, there is a critical need for new types of climate reconstructions that span the Holocene.

In the Kangerlussuaq region of southwest Greenland (Figure 1), extensive moraine systems (Lesnek & Briner, 2018; Ten Brink, 1975) formed during short-lived cooling events (e.g., the 9.3 and 8.2 ka events; Young et al., 2020). The sensitivity of this land-based Greenland Ice Sheet (GrIS) sector to abrupt climatic change suggests the ice margin was in nearequilibrium with climate throughout the Holocene. Because the GrIS in this area is not heavily influenced by ice dynamics (e.g., calving; Csatho et al., 2014) and the ice margin has a relatively short response time (Young et al., 2020), its retreat history can be used as a proxy for surface mass balance, which is closely tied to summer temperature and winter precipitation (Cuzzone et al., 2019). Here we synthesize new and previously published chronologies to reconstruct the spatial pattern of GrIS change in the Kangerlussuaq region over the past ~12 ka. We then discuss the history of this ice sheet sector in the broader context of the HTM.

2. Materials and Methods

We compiled published age constraints that relate to the timing of southwest GrIS margin change. Of these ages, 295 are cosmogenic ^{10}Be surface exposure ages, which directly date deglaciation, and 189 are minimum- or maximum-limiting ^{14}C ages from lake sediments ($n = 79$), marine shells ($n = 109$), or benthic foraminifera ($n = 1$). We also generated 13 new ^{14}C ages from sediments in eight proglacial lakes (supporting information). All ^{10}Be ages were (re)calculated with version 3 of the CRONUS Earth calculator (hess.ess.washington.edu; Balco, 2017; Balco et al., 2008) using the Baffin Bay/Arctic production rate (Young, Schaefer, et al., 2013) and Lm scaling (Lal, 1991; Stone, 2000), which is commonly used to calculate ^{10}Be exposure ages in Greenland (e.g., Lesnek & Briner, 2018; Winsor, Carlson, Caffee, et al., 2015). However, for comparison with other production rates and scaling schemes, we have made available all information needed to recalculate the ^{10}Be exposure ages at the NOAA National Centers for Environment Information (https://www.ncdc.noaa.gov/paleo-search/study/26450). All ^{14}C ages were (re)calculated in OxCal version 4.3 (Bronk Ramsey, 2009, 2017). Marine ^{14}C ages were corrected using a total marine reservoir age of 540 ± 35 years ($\Delta R = 140 \pm 35$ years; Lloyd et al., 2011).

We combined the chronology compilation and the ArcticDEM (Porter et al., 2018) to map Holocene ice margin positions from ~71°N to 64°N. Our mapping builds on previous work by Weidick (1974), who mapped Quaternary surficial deposits across West Greenland. Using our chronology compilation, we mapped the moraine systems by age and correlated them across the entire study area, interpolating ice margin positions between areas without well-preserved moraine crests. Moraine locations were field verified in Jakobshavn (Young et al., 2011; Young, Briner, et al., 2013), Naternaq (Kelley et al., 2015), Kangerlussuaq (Young et al., 2020), Søndre Isortoq (Lesnek & Briner, 2018), and Kangersuneq (Figure S1).

We then used the ice margin map to reconstruct Holocene retreat rates on a land-based GrIS sector in the Kangerlussuaq region (Figure 1). We focused these efforts specifically on the Kangerlussuaq region, rather than the broader southwestern GrIS, for several reasons. First, in ice sheet regions dominated by surface mass balance (Cuzzone et al., 2019; Sole et al., 2008), the rate of ice margin change is related to climate forcing on centennial-to-millennial timescales (Kelley et al., 2015). The retreat history of land-based GrIS sectors, such as the Kangerlussuaq region, can therefore provide insight into climatic conditions over the Holocene. Second, a suite of five early Holocene moraine systems are preserved throughout the region (Figure 1), and the age of each ice margin position is directly constrained by ^{10}Be ages from moraine boulders ($n = 60$; Carlson et al., 2014; Levy et al., 2012; Winsor, Carlson, Welke, et al., 2015; Young et al., 2020) and supported by the broader chronology compilation. Finally, Holocene ice-margin recession in this region was not impacted by re-advances over large distances. Maximum-limiting ^{10}Be ages from perched boulders outside of the Taserqat, Sarfartôq-Avadtleq, Fjord, and Ørkendalen moraine systems are statistically indistinguishable from moraine boulder ^{10}Be ages (Young et al., 2020), indicating that the moraines were deposited during ice margin stillstands. Thus, the measured retreat rates for this GrIS sector closely correspond to "true" ice margin retreat rates. We calculated linear retreat rates along east-west trending profile lines that intersect mapped ice margin positions (Figure 1). Linear retreat rates are reported in m a^{-1}. To assess possible differences in retreat due to aclimatic (e.g., topographic) factors, we divided the study region into uniform zones that encompass 15 min of latitude and 5° of longitude (Figure 1), created swath topographic profiles (supporting information Text S2.3), and calculated the area (not considering surface topography) between each dated moraine stage. We then calculated the area-integrated retreat rate between the moraine stages in each zone, which is reported in m^2 a^{-1}.

We used ^{14}C ages from proglacial threshold lake sediments (Briner et al., 2010) to estimate the timing and extent of inland retreat during the middle Holocene from 11 new lake sediment cores. During intervals when the GrIS is at or near its current extent, these lakes receive ice sheet meltwater, and silt-rich sediments are deposited in the lake basin. Once the ice margin recedes behind a topographic threshold (derived from BedMachine v3; Morlighem et al., 2017), ice sheet meltwater no longer reaches the lake basin and accumulation of organic-rich sediment (gyttja) begins. By ^{14}C-dating the contacts between major sediment transitions, we constrain the age of GrIS movement into and out of a lake's catchment (e.g., Bjørk et al., 2018; Håkansson et al., 2014; Larsen et al., 2015; Young et al., 2011). To estimate the timing of minimum ice extent, we calculated the midpoint between basal and upper ^{14}C ages and estimated the magnitude of inland recession by assuming the ice margin maintained a constant retreat rate between the abandonment of the Ørkendalen moraines at ~7.3 ka and the basal ^{14}C ages (see supporting information).
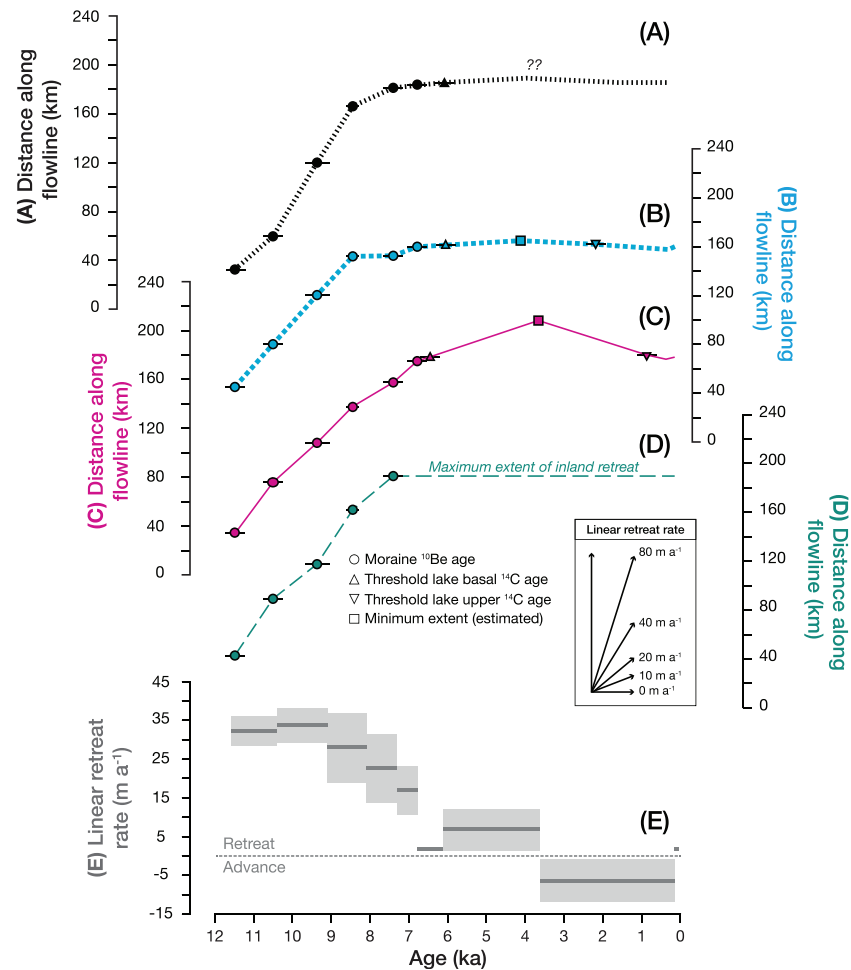
Figure 2. (a–d) Linear retreat rates in the Kangerlussuaq region along profiles with proglacial threshold lakes: Four Hare Lake (a), Lake Lucy (b), Baby Loon Lake (c), and Tasersuaq (d). Circles represent [10]Be ages from moraine systems (Carlson et al., 2014; Levy et al., 2012; Winsor, Carlson, Caffee, et al., 2015; Young et al., 2020). Triangles indicate ^{14}C ages from proglacial threshold lakes. Squares indicate the estimated extent of inland GrIS retreat. (e) Average linear retreat rates for the four profiles. Dark gray lines represent average retreat rates per time interval and shading indicates the standard error of the mean.

3. Results

We report six new ^{14}C ages from four proglacial threshold lakes in the Kangerlussuaq region. Basal ^{14}C ages from the contact between basal silt-rich and overlying organic-rich sediments, which represent the time when the GrIS margin retreated from each lake's catchment, range from $5,980 \pm 320$ to $6,050 \pm 120$ cal year BP ($n = 4$). Upper ^{14}C ages at or very near the transition from organic-rich to mineral-rich sediments ($n = 2$) that record the GrIS advance back into the lake catchments are 690 ± 20 and $1,450 \pm 150$ cal year BP (see supporting information). In the Kangersuneq region (Figure S1), new basal ^{14}C ages from four proglacial threshold lakes range from $7,490 \pm 70$ to $9,160 \pm 130$ cal year BP ($n = 3$). Upper ages from these lakes range from 490 ± 20 to 940 ± 20 cal year BP ($n = 4$).

Combining the lake sediment constraints with early Holocene ice margin positions (Figure 1) allowed us to calculate linear GrIS retreat rates between 11.6 and 0 ka (Figure 2). We also calculated area-integrated retreat rates for four intervals that are bracketed by the five dated moraine systems (Figure 3 and Table S4). Area-integrated retreat rates between 11.6 and 10.4 ka average $7.0 \pm 2.7 \times 10^5$ m^2 a^{-1}. From 10.4 to 9.1 ka, the net retreat rate increased to $10.7 \pm 3.7 \times 10^5$ m^2 a^{-1}. Between 9.1 and 8.1 ka, net retreat rates decreased to $7.5 \pm 4.3 \times 10^5$ m^2 a^{-1}, and GrIS retreat rates slowed further between 8.1 and 7.3 ka, averaging $3.7 \pm 2.7 \times 10^5$ m^2 a^{-1}.
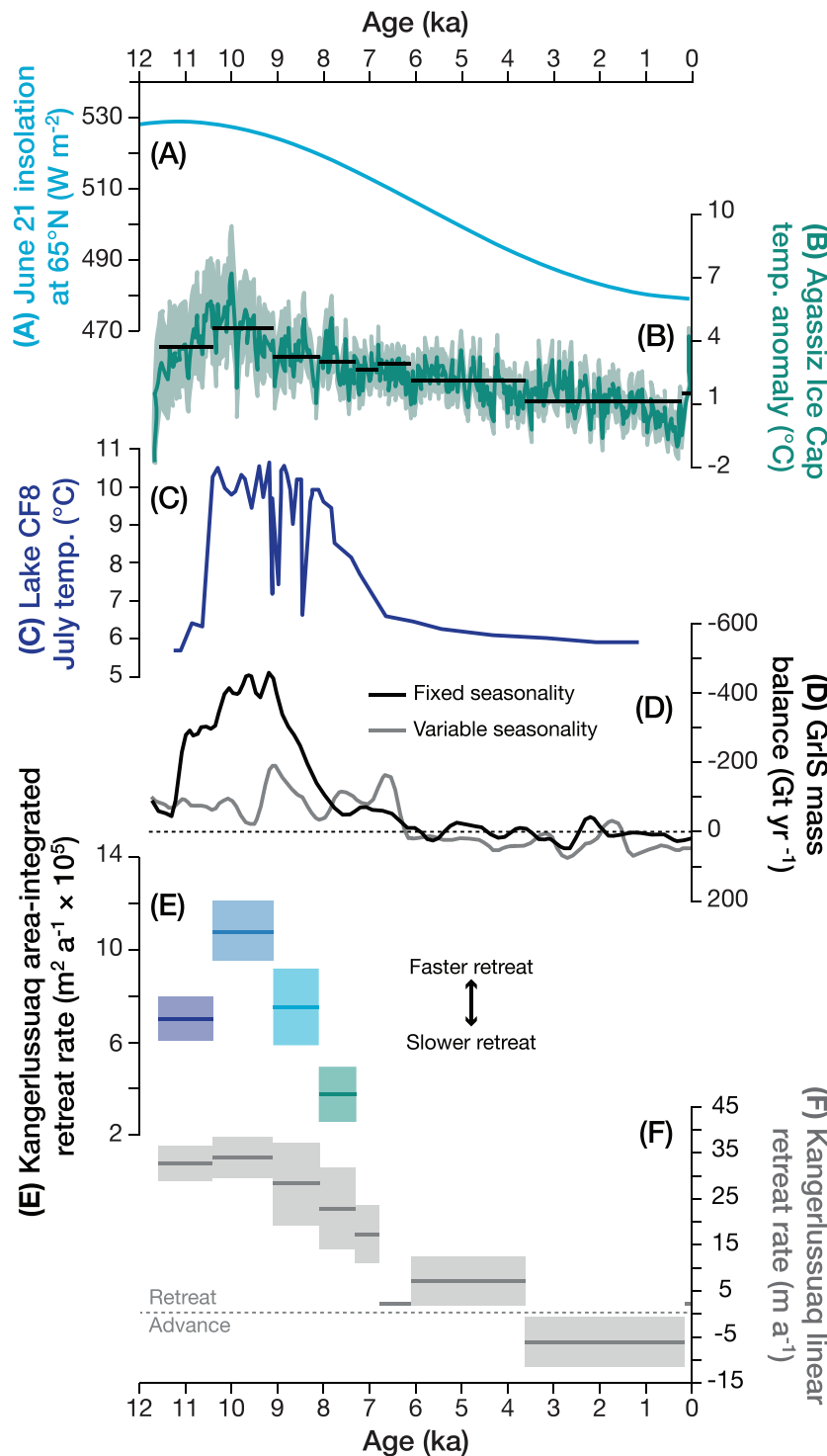
Figure 3. (a) June 21 insolation at 65°N (Laskar et al., 2004). (b) Holocene temperature anomalies (relative to 1750 CE) derived from $\delta^{18}O$ in the Agassiz Ice Cap (Lecavalier et al., 2017). Dark green line shows average temperature and light green shading represents 2σ uncertainty. For comparison with panels (e) and (f), solid black lines depict average temperatures for the time periods bracketed by the moraine system ^{10}Be ages and/or threshold lake ^{14}C ages. (c) Chironomid-derived July temperature reconstruction from Lake CF8, eastern Baffin Island (Axford et al., 2009). (d) Simulated GrIS mass balance forced by fixed (relative to modern; black line) and variable (gray line) temperature seasonality (Buizert et al., 2018). Note the inverted y axis. (e) Area-integrated GrIS retreat rates. Solid lines are average values for all areas, color coded by age, and the shading around each line represents the standard error of the mean. (f) Average linear retreat rates along profiles for Four Hare Lake, Lake Lucy, Baby Loon Lake, and Tasersuaq. Dark gray lines represent average retreat rates per time interval and shading indicates the standard error of the mean.

We investigated the relationship between topography and ice margin retreat, and based on our swath topography analysis, we found no relationship between area-integrated retreat rates and topography (Figure S11). It is possible that there were intervals between moraine positions with higher retreat rates than were calculated here. Thus, the area-integrated retreat rates presented here should be viewed as minimum estimates.

Basal ages from proglacial threshold lakes reveal an additional decrease in retreat rates after 7.3 ka (Figure 2). The sub-ice drainage basin threshold for Four Hare Lake lies ~1 km behind the 2001 GrIS margin. A basal ^{14}C age from a core collected from this lake indicates the GrIS first retreated out of Four Hare Lake's catchment at $6,060 \pm 120$ cal year BP. The calculated linear retreat rate between the Ørkendalen moraines and GrIS retreat out of Four Hare Lake's sub-ice catchment was 2.0 m a^{-1} (Figure 2a).

At Lake Lucy, the sub-ice drainage basin threshold extends ~0.9 km behind the 2001 margin (Young & Briner, 2015). The GrIS retreated out of Lake Lucy's catchment at $6,050 \pm 60$ cal year BP, remaining behind the topographic threshold until $1,450 \pm 150$ cal year BP. We estimate that the ice margin in this zone retreated ~3.7 km inland of its modern configuration and reached this minimum position at ~3.8 ka. Between the Ørkendalen moraines and Lake Lucy's sub-ice threshold, the net retreat rate was 1.2 m a^{-1} (Figure 2b).

The sub-ice threshold for Baby Loon Lake lies ~1 km behind the 2001 GrIS margin. Transitions between mineral-rich and organic-rich sediments occurred at $6,370 \pm 130$ and 690 ± 20 cal year BP. We estimate that the ice margin in this zone retreated ~26 km inland of its current position and achieved this extent at ~3.5 ka. Between the Ørkendalen moraines and Baby Loon Lake's threshold, the net retreat rate was 12.0 m a^{-1} (Figure 2c).

Tasersuaq is a proglacial lake that lies ~40 km west of the modern GrIS and whose sub-ice drainage basin extends ~1.9 km inland of the GrIS margin. A shift in sedimentation at $5,980 \pm 320$ cal year BP, from glacially derived mineral-rich sediments to silty gyttja that extends to the surface, marks an interval of lake inflow reorganization and suggests that ice margin never retreated entirely from Tasersuaq's drainage basin after ~6 ka (see supporting information). Based on this inference, we suggest that in this location, the GrIS retreated no more than ~1.9 km inland its present position during the middle Holocene, and net retreat rates did not exceed 0.6 m a^{-1} (Figure 2d).

4. Holocene Retreat Rates of the Western Greenland Ice Sheet

We observe increasing retreat rates through the earliest Holocene, with maximum Holocene GrIS recession occurring between ~10.4 and 9.1 ka (Figure 3). After this interval, GrIS retreat rates decreased until they reached a minimum after ~7.3 ka. This decrease in retreat rates led to minimal inland recession during the middle Holocene, in most cases less than 4 km. Deceleration of GrIS retreat in the middle Holocene has been observed along other land-based margins in southwest Greenland (Figure S1), including Paakitsoq (Håkansson et al., 2014), Nuussuaq (Cronauer et al., 2016), and Isua (Levy et al., 2017). In the Kangerlussuaq region, geophysical surveys reveal that sub-icesheet permafrost, which can only form when an area is deglaciated, extends just ~2 km inland of the GrIS terminus near Issunguata Sermia (Ruskeeniemi et al., 2018). Ice-dammed basin sediments near the Russell Glacier further constrain the timing of restricted ice extent to a relatively narrow window between ~6.8 and 4.2 ka (Carrivick et al., 2018). Thus, the collective evidence suggests that land-based southwest GrIS margins experienced a major slowdown in retreat rates after ~7 ka.

The coherence in moraine system ages across southwestern Greenland points to a climatic forcing of GrIS change during the Holocene (Young, Briner, et al., 2013). In turn, rapid and widespread GrIS response to Holocene cooling events (Young et al., 2020) suggests that the southwest GrIS margin was in balance with climate and was not retreating in the early Holocene simply as a lagged response to latest Pleistocene warming (Buizert et al., 2018; Shakun et al., 2012). We also find that topography was not a major influence on area-integrated retreat rates (Figure S11), further emphasizing the role of climate in driving GrIS recession. Assuming that this sector of the GrIS was in equilibrium with Holocene climate, periods with high retreat rates should indicate intervals with persistent negative mass balance. Indeed, the fastest reconstructed ice margin recession occurred during a time of intense mass loss in simulations of GrIS-wide mass balance (e.g., Buizert et al., 2018; Figure 3). Furthermore, both the Huy3 (Lecavalier et al., 2014) and Buizert et al.
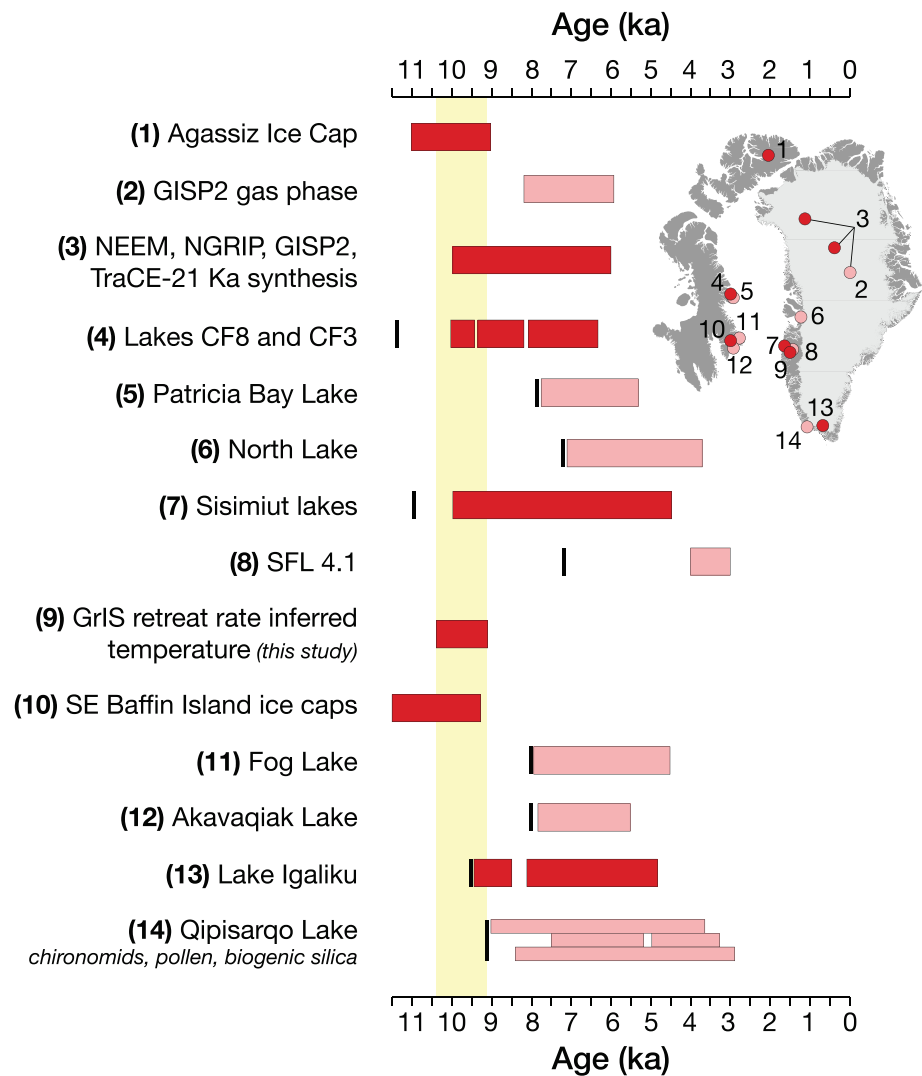
Figure 4. Timing of the HTM across the Baffin Bay region (adapted from Briner et al., 2016). Vertical yellow bar denotes the period of maximum southwest GrIS recession (10.4–9.1 ka). Horizontal red bars (and dots on inset map) represent sites with an early HTM; pink bars (and dots on inset map) are sites with a late HTM. Black bars indicate the onset of non-glacial lacustrine sedimentation or the base of sediment cores. Refer to text for site sources.

(2018) models simulate a transition from negative to near-zero mass balance at ~6.5 ka, consistent with our finding of reduced ice margin recession after ~7 ka.

Model simulations suggest that the principal control on mass balance in land-based ice sheet areas in southwest Greenland is summer temperature (Cuzzone et al., 2019; Schlegel et al., 2016). Low levels of winter precipitation may also contribute to fast ice recession and, conversely, increased snowfall during periods of warmth has been hypothesized to partially offset temperature-driven mass loss (Thomas et al., 2016). However, numerical modeling indicates that warming of ~2 °C above modern mean annual air temperature is capable of producing sufficient melt to outpace mass gains from increased accumulation (Rae et al., 2012). This modest temperature increase is similar in magnitude to estimates of Arctic-wide warming during the HTM (Kaufman et al., 2004). Therefore, our results suggest that in southwest Greenland, the warmest summer air temperatures over the entire Holocene occurred between ~10.4 and 9.1 ka.

Resolving the timing of the HTM in the Arctic has been the focus of numerous studies, and recent syntheses (Briner et al., 2016; Kaufman et al., 2004) have highlighted considerable discrepancies in climate reconstructions across the Baffin Bay region (Figure 4). Records from eastern Baffin Island (Lakes CF8 and CF3; Axford et al., 2009), south Greenland (Lake Igaliku; Massa et al., 2012), the Sisimiut region (Wagner &

Bennike, 2012), southeast Baffin Island ice caps (Pendleton et al., 2019), and the Agassiz Ice Cap (Bourgeois et al., 2000; Fisher et al., 2012; Lecavalier et al., 2017) suggest the warmest millennia of the Holocene occurred before ~8 ka, coincident with maximum summer insolation (Figure 3). Yet reconstructions from chironomid assemblages (North Lake; Axford et al., 2013), pollen (Patricia Bay and Fog Lakes; Fréchette et al., 2006; Gajewski, 2015; Kerwin et al., 2004), the GISP2 ice core (Kobashi et al., 2017), and lake sediments (Akavaqiak Lake and SFL 4.1; Fréchette & Vernal, 2009; Willemse & Tornqvist, 1999) suggest that maximum air temperatures lagged peak insolation by several millennia. However, many reconstructions that identify a late HTM do not extend to the earliest Holocene (Figure 4), leaving open the possibility of an earlier period of maximum warmth that is not captured by these shorter records. Although ice cores provide continuous, long-term climate information, reconstructions from the GrIS divide (e.g., Alley & Anandakrishnan, 1995; Kobashi et al., 2017), which suggest peak warmth in the middle Holocene (Figure 4), may not reflect climatic conditions at the margins, especially when considering the complication of core site elevation change through time (Vinther et al., 2009). Indeed, merging multiple ice core reconstructions with transient climate simulations produces an expanded interval of elevated summer air temperatures, spanning from ~10 to 6.5 ka (Figure 4; Buizert et al., 2018), which is broadly consistent with our results from southwest Greenland. In summary, our record of GrIS margin change over the past ~12 ka supports an early HTM in the Baffin Bay region and demonstrates the advantage of Holocene-length temperature reconstructions for addressing questions about long-term regional climate trends.

5. Conclusions

Our compilation of 497 [10]Be and ^{14}C ages from southwest Greenland allowed us to (1) generate a complete reconstruction of GrIS margin positions between ~12 and 7 ka, (2) estimate ice margin positions after ~7 ka, and thus (3) constrain net ice sheet retreat rates over the entire Holocene. Within this context, maximum southwest GrIS recession occurred between ~10.4 and 9.1 ka, and retreat rates likely reached a minimum after ~7.3 ka. The lack of a relationship between net retreat rates and landscape-scale topography and the widespread existence of moraines that date to short-lived cooling events both implicate regional climate as the primary driver of southwest GrIS margin change over the past ~12 ka. The tight coupling of land-based GrIS margins to Holocene climate suggests that the summer air temperatures in southwest Greenland were highest from ~10.4 to 9.1 ka, providing independent support for an early HTM in the Baffin Bay region. Finally, our reconstruction offers new, geologically constrained targets that can be used to assess ice sheet and climate model performance over the Holocene.

References

Alley, R. B., & Anandakrishnan, S. (1995). Variations in melt-layer frequency in the GISP2 ice core: Implications for Holocene summer temperatures in central Greenland. *Annals of Glaciology*, *21*, 64–70.

Axford, Y., Briner, J. P., Miller, G. H., & Francis, D. R. (2009). Paleoecological evidence for abrupt cold reversals during peak Holocene warmth on Baffin Island, Arctic Canada. *Quaternary Research*, *71*(2), 142–149.

Axford, Y., Losee, S., Briner, J. P., Francis, D. R., Langdon, P. G., & Walker, I. R. (2013). Holocene temperature history at the western Greenland ice sheet margin reconstructed from lake sediments. *Quaternary Science Reviews*, *59*, 87–100.

Balco, G. (2017). Production rate calculations for cosmic-ray-muon-produced [10]Be and [26]Al benchmarked against geological calibration data. *Quaternary Geochronology*, *39*, 150–173. https://doi.org/10.1016/j.quageo.2017.02.001

Balco, G., Stone, J. O., Lifton, N. A., & Dunai, T. J. (2008). A complete and easily accessible means of calculating surface exposure ages or erosion rates from [10]Be and [26]Al measurements. *Quaternary Geochronology*, *3*(3), 174–195.

Bjørk, A., Larsen, N., Olsen, J., Goldsack, A., Kjeldsen, K., Morlighem, M., et al. (2018). Holocene history of the Helheim Glacier, southeast Greenland. *Quaternary Science Reviews*, *193*, 145–158. https://doi.org/10.1016/j.quascirev.2018.06.018

Bourgeois, J. C., Koerner, R. M., Gajewski, K., & Fisher, D. A. (2000). A Holocene ice-core pollen record from Ellesmere Island, Nunavut, Canada. *Quaternary Research*, *54*(2), 275–283.

Briner, J. P., McKay, N. P., Axford, Y., Bennike, O., Bradley, R. S., de Vernal, A., et al. (2016). Holocene climate change in Arctic Canada and Greenland. *Quaternary Science Reviews*, *147*, 340–364. https://doi.org/10.1016/j.quascirev.2016.02.010

Briner, J. P., Stewart, H. A. M., Young, N. E., Philipps, W., & Losee, S. (2010). Using proglacial-threshold lakes to constrain fluctuations of the Jakobshavn Isbræ ice margin, western Greenland, during the Holocene. *Quaternary Science Reviews*, *29*(27–28), 3861–3874.

Bronk Ramsey, C. (2009). Bayesian analysis of radiocarbon dates. *Radiocarbon*, *51*(1), 337–360.

Bronk Ramsey, C. (2017). Methods for summarizing radiocarbon datasets. *Radiocarbon*, *59*(6), 1809–1833.

Buizert, C., Keisling, B., Box, J., He, F., Carlson, A., Sinclair, G., & DeConto, R. (2018). Greenland-wide seasonal temperatures during the last deglaciation. *Geophysical Research Letters*, *45*, 1905–1914. https://doi.org/10.1002/2017GL075601

Carlson, A. E., Winsor, K., Ullman, D. J., Brook, E. J., Rood, D. H., Axford, Y., et al. (2014). Earliest Holocene south Greenland ice sheet retreat within its late Holocene extent. *Geophysical Research Letters*, *41*, 5514–5521. https://doi.org/10.1002/2014GL060800

Carrivick, J. L., Yde, J. C., Knudsen, N. T., & Kronborg, C. (2018). Ice-dammed lake and ice-margin evolution during the Holocene in the Kangerlussuaq area of west Greenland. *Arctic, Antarctic, and Alpine Research*, *50*(1), S100005.

Cronauer, S. L., Briner, J. P., Kelley, S. E., Zimmerman, S. R. H., & Morlighem, M. (2016). [10]Be dating reveals early-middle Holocene age of the Drygalski Moraines in central West Greenland. *Quaternary Science Reviews*, *147*, 59–68.

Csatho, B. M., Schenk, A. F., van der Veen, C. J., Babonis, G., Duncan, K., Rezvanbehbahani, S., et al. (2014). Laser altimetry reveals complex pattern of Greenland ice sheet dynamics. *Proceedings of the National Academy of Sciences*, *111*(52), 18478–18483. https://doi.org/10.1073/pnas.1411680112

Cuzzone, J. K., Schlegel, N. J., Morlighem, M., Larour, E., Briner, J. P., Seroussi, H., & Caron, L. (2019). The impact of model resolution on the simulated Holocene retreat of the southwestern Greenland ice sheet using the Ice Sheet System Model (ISSM). *The Cryosphere*, *13*(3), 879–893.

Fisher, D., Zheng, J., Burgess, D., Zdanowicz, C., Kinnard, C., Sharp, M., & Bourgeois, J. (2012). Recent melt rates of Canadian arctic ice caps are the highest in four millennia. *Global and Planetary Change*, *84*, 3–7.

Fréchette, B., & Vernal, A. d. (2009). Relationship between Holocene climate variations over southern Greenland and eastern Baffin Island and synoptic circulation pattern. *Climate of the Past*, *5*(3), 347–359.

Fréchette, B., Wolfe, A. P., Miller, G. H., Richard, P. J., & de Vernal, A. (2006). Vegetation and climate of the last interglacial on Baffin Island, Arctic Canada. *Palaeogeography, Palaeoclimatology, Palaeoecology*, *236*(1-2), 91–106.

Gajewski, K. (2015). Quantitative reconstruction of Holocene temperatures across the Canadian Arctic and Greenland. *Global and Planetary Change*, *128*, 14–23.

Håkansson, L., Briner, J. P., Andresen, C. S., Thomas, E. K., & Bennike, O. (2014). Slow retreat of a land based sector of the west Greenland ice sheet during the Holocene thermal maximum: Evidence from threshold lakes at Paakitsoq. *Quaternary Science Reviews*, *98*, 74–83.

Kaufman, D. S., Ager, T. A., Anderson, N. J., Anderson, P. M., Andrews, J. T., Bartlein, P. J., et al. (2004). Holocene thermal maximum in the western Arctic (0–180°W). *Quaternary Science Reviews*, *23*(5–6), 529–560. https://doi.org/10.1016/j.quascirev.2003.09.007

Kelley, S. E., Briner, J. P., & Zimmerman, S. R. (2015). The influence of ice marginal setting on early Holocene retreat rates in central West Greenland. *Journal of Quaternary Science*, *30*(3), 271–280.

Kerwin, M. W., Overpeck, J. T., Webb, R. S., & Anderson, K. H. (2004). Pollen-based summer temperature reconstructions for the eastern Canadian boreal forest, subarctic, and Arctic. *Quaternary Science Reviews*, *23*(18-19), 1901–1924.

Kobashi, T., Menviel, L., Jeltsch-Thömmes, A., Vinther, B. M., Box, J. E., Muscheler, R., et al. (2017). Volcanic influence on centennial to millennial Holocene Greenland temperature change. *Scientific Reports*, *7*(1), 1441. https://doi.org/10.1038/s41598-017-01451-7

Lal, D. (1991). Cosmic ray labeling of erosion surfaces: In situ nuclide production rates and erosion models. *Earth and Planetary Science Letters*, *104*(2-4), 424–439.

Larsen, N. K., Kjær, K. H., Lecavalier, B., Bjørk, A. A., Colding, S., Huybrechts, P., et al. (2015). The response of the southern Greenland ice sheet to the Holocene thermal maximum. *Geology*, *43*(4), 291–294. https://doi.org/10.1130/G36476.1

Laskar, J., Robutel, P., Joutel, F., Gastineau, M., Correia, A., & Levrard, B. (2004). A long-term numerical solution for the insolation quantities of the Earth. *Astronomy & Astrophysics*, *428*(1), 261–285.

Lecavalier, B. S., Fisher, D. A., Milne, G. A., Vinther, B. M., Tarasov, L., Huybrechts, P., et al. (2017). High Arctic Holocene temperature record from the Agassiz ice cap and Greenland ice sheet evolution. *Proceedings of the National Academy of Sciences*, 201616287.

Lecavalier, B. S., Milne, G. A., Simpson, M. J., Wake, L., Huybrechts, P., Tarasov, L., et al. (2014). A model of Greenland ice sheet deglaciation constrained by observations of relative sea level and ice extent. *Quaternary Science Reviews*, *102*, 54–84. https://doi.org/10.1016/j.quascirev.2014.07.018

Lesnek, A. J., & Briner, J. P. (2018). Response of a land-terminating sector of the western Greenland ice sheet to early Holocene climate change: Evidence from [10]Be dating in the Søndre Isortoq region. *Quaternary Science Reviews*, *180*, 145–156.

Levy, L., Larsen, N., Davidson, T., Strunk, A., Olsen, J., & Jeppesen, E. (2017). Contrasting evidence of Holocene ice margin retreat, southwestern Greenland. *Journal of Quaternary Science*, *32*(5), 604–616.

Levy, L. B., Kelly, M. A., Howley, J. A., & Virginia, R. A. (2012). Age of the Orkendalen moraines, Kangerlussuaq, Greenland: Constraints on the extent of the southwestern margin of the Greenland ice sheet during the Holocene. *Quaternary Science Reviews*, *52*, 1–5.

Lloyd, J., Moros, M., Perner, K., Telford, R. J., Kuijpers, A., Jansen, E., & McCarthy, D. (2011). A 100 yr record of ocean temperature control on the stability of Jakobshavn Isbrae, West Greenland. *Geology*, *39*(9), 867–870.

Lloyd, J., Park, L., Kuijpers, A., & Moros, M. (2005). Early Holocene palaeoceanography and deglacial chronology of Disko Bugt, west Greenland. *Quaternary Science Reviews*, *24*(14-15), 1741–1755. Massa, C., Perren, B. B., Gauthier, E., Bichet, V., Petit, C., & Richard, H. (2012). A multiproxy evaluation of Holocene environmental change from Lake Igaliku, South Greenland. *Journal of Paleolimnology*, *48*(1), 241–258.

McKay, N. P., Kaufman, D. S., Routson, C. C., Erb, M. P., & Zander, P. D. (2018). The onset and rate of Holocene Neoglacial cooling in the Arctic. *Geophysical Research Letters*, *45*, 12,487–412,496. https://doi.org/10.1029/2018GL079773

Morlighem, M., Williams, C. N., Rignot, E., An, L., Arndt, J. E., Bamber, J. L., et al. (2017). BedMachine v3: Complete bed topography and ocean bathymetry mapping of Greenland from multibeam echo sounding combined with mass conservation. *Geophysical Research Letters*, *44*, 11,051–11,061. https://doi.org/10.1002/2017GL074954

Pendleton, S., Miller, G., Lifton, N., & Young, N. (2019). Cryosphere response resolves conflicting evidence for the timing of peak Holocene warmth on Baffin Island, Arctic Canada. *Quaternary Science Reviews*, *216*, 107–115.

Porter, C., Morin, P., Howat, I., Noh, M.-J., Bates, B., Peterman, K., et al. (2018). *ArcticDEM* [Digital Elevation Model]. Retrieved from: https://doi.org/10.7910/DVN/OHHUKH

Quillmann, U., Andrews, J. T., Jennings, A. E., Bendle, J., Jonsdottir, H., Kristjansdottir, G., et al. (2009). Radiocarbon date list XI: Radiocarbon dates from marine sediment cores of the Iceland, Greenland, and Northeast Canadian Arctic Shelves and Nares Strait.

Rae, J., Aðalgeirsdóttir, G., Edwards, T., Fettweis, X., Gregory, G., Hewitt, H., et al. (2012). Greenland ice sheet surface mass balance: Evaluating simulations and making projections with regional climate models. *Cryosphere (The)*, *6*(6), 1275–1294. https://doi.org/10.5194/tc-6-1275-2012

Ruskeeniemi, T., Engström, J., Lehtimäki, J., Vanhala, H., Korhonen, K., Kontula, A., et al. (2018). Subglacial permafrost evidencing readvance of the Greenland ice sheet over frozen ground. *Quaternary Science Reviews*, *199*, 174–187. https://doi.org/10.1016/j.quascirev.2018.09.002

Schlegel, N., Wiese, D., Larour, E., Watkins, M., Box, J., Fettweis, X., & van den Broeke, M. (2016). Application of GRACE to the assessment of model-based estimates of monthly Greenland ice sheet mass balance (2003–2012). *Cryosphere (The)*, *10*, 1965–1989.

Shakun, J. D., Clark, P. U., He, F., Marcott, S. A., Mix, A. C., Liu, Z., et al. (2012). Global warming preceded by increasing carbon dioxide concentrations during the last deglaciation. *Nature*, *484*(7392), 49–54. https://doi.org/10.1038/nature10915

Sole, A., Payne, T., Bamber, J., Nienow, P., & Krabill, W. (2008). Testing hypotheses of the cause of peripheral thinning of the Greenland ice sheet: Is land-terminating ice thinning at anomalously high rates? *The Cryosphere*, *2*(2), 205–218.

Stone, J. O. (2000). Air pressure and cosmogenic isotope production. *Journal of Geophysical Research*, *105*(B10), 23753–23759.

Ten Brink, N. W. (1975). Holocene history of the Greenland ice sheet based on radiocarbon-dated moraines in West Greenland. *Meddelelser om Grønland*, *44*(113).

Thomas, E. K., Briner, J. P., Ryan-Henry, J. J., & Huang, Y. (2016). A major increase in winter snowfall during the middle Holocene on western Greenland caused by reduced sea ice in Baffin Bay and the Labrador Sea. *Geophysical Research Letters*, *43*, 5302–5308. https://doi.org/10.1002/2016GL068513

Vinther, B. M., Buchardt, S. L., Clausen, H. B., Dahl-Jensen, D., Johnsen, S. J., Fisher, D., et al. (2009). Holocene thinning of the Greenland ice sheet. *Nature*, *461*(7262), 385–388. https://doi.org/10.1038/nature08355

Wagner, B., & Bennike, O. (2012). Chronology of the last deglaciation and Holocene environmental changes in the Sisimiut area, SW Greenland based on lacustrine records. *Boreas*, *41*(3), 481–493.

Weidick, A. (1974). *Quaternary map of Greenland, 1: 500 000, Søndre Strømfjord–Nûgssuaq, sheet 3*. Copenhagen: Geological Survey of Greenland.

Willemse, N. W., & Tornqvist, T. E. (1999). Holocene century-scale temperature variability from West Greenland lake records. *Geology*, *27*(7), 580–584.

Winsor, K., Carlson, A. E., Caffee, M. W., & Rood, D. H. (2015). Rapid last-deglacial thinning and retreat of the marine-terminating southwestern Greenland ice sheet. *Earth and Planetary Science Letters*, *426*, 1–12.

Winsor, K., Carlson, A. E., Welke, B. M., & Reilly, B. (2015). Early deglacial onset of southwestern Greenland ice-sheet retreat on the continental shelf. *Quaternary Science Reviews*, *128*, 117–126.

Young, N. E., & Briner, J. P. (2015). Holocene evolution of the western Greenland ice sheet: Assessing geophysical ice-sheet models with geological reconstructions of ice-margin change. *Quaternary Science Reviews*, *114*, 1–17.

Young, N. E., Briner, J. P., Axford, Y., Csatho, B., Babonis, G. S., Rood, D. H., & Finkel, R. C. (2011). Response of a marine-terminating Greenland outlet glacier to abrupt cooling 8200 and 9300 years ago. *Geophysical Research Letters*, *38*, L24701. https://doi.org/10.1029/2011GL049639

Young, N. E., Briner, J. P., Miller, G. H., Lesnek, A. J., Crump, S. E., Thomas, E. K., et al. (2020). Deglaciation of the Greenland and Laurentide ice sheets interrupted by glacier advance during abrupt coolings. *Quaternary Science Reviews*, *229*, 106091. https://doi.org/10.1016/j.quascirev.2019.106091

Young, N. E., Briner, J. P., Rood, D. H., Finkel, R. C., Corbett, L. B., & Bierman, P. R. (2013). Age of the Fjord Stade moraines in the Disko Bugt region, western Greenland, and the 9.3 and 8.2 ka cooling events. *Quaternary Science Reviews*, *60*, 76–90.

Young, N. E., Schaefer, J. M., Briner, J. P., & Goehring, B. M. (2013). A ^{10}Be production-rate calibration for the Arctic. *Journal of Quaternary Science*, *28*(5), 515–526.

References From the Supporting Information

Bennike, O., & Björck, S. (2002). Chronology of the last recession of the Greenland ice sheet. *Journal of Quaternary Science*, *17*(3), 211–219.

Bennike, O., Wagner, B., & Richter, A. (2011). Relative sea level changes during the Holocene in the Sisimiut area, south-western Greenland. *Journal of Quaternary Science*, *26*(4), 353–361.

Briner, J. P., Håkansson, L., & Bennike, O. (2013). The deglaciation and neoglaciation of Upernavik Isstrøm, Greenland. *Quaternary Research*, *80*(3), 459–467.

Briner, J. P., Kaufman, D. S., Bennike, O., & Kosnik, M. A. (2014). Amino acid ratios in reworked marine bivalve shells constrain Greenland ice sheet history during the Holocene. *Geology*, *42*(1), 75–78.

Corbett, L. B., Bierman, P. R., Graly, J. A., Neumann, T. A., & Rood, D. H. (2013). Constraining landscape history and glacial erosivity using paired cosmogenic nuclides in Upernavik, northwest Greenland. *Geological Society of America Bulletin*, *125*(9-10), 1539–1553.

Corbett, L. B., Young, N. E., Bierman, P. R., Briner, J. P., Neumann, T. A., Rood, D. H., & Graly, J. A. (2011). Paired bedrock and boulder ^{10}Be concentrations resulting from early Holocene ice retreat near Jakobshavn Isfjord, western Greenland. *Quaternary Science Reviews*, *30*(13), 1739–1749.

Eisner, W. R., Törnqvist, T. E., Koster, E. A., Bennike, O., & van Leeuwen, J. F. (1995). Paleoecological studies of a Holocene lacustrine record from the Kangerlussuaq (Søndre Strømfjord) region of West Greenland. *Quaternary Research*, *43*(1), 55–66.

Fredskild, B. (1983). *The Holocene vegetational development of the Godthåbsfjord area, West Greenland*, Commission for Scientific Research in Greenland (Vol. 10). Copenhagen, Denmark: Meddelelser om Grønland.

Hogan, K. A., Cofaigh, C. Ó., Jennings, A. E., Dowdeswell, J. A., & Hiemstra, J. F. (2016). Deglaciation of a major palaeo-ice stream in Disko Trough, West Greenland. *Quaternary Science Reviews*, *147*, 5–26.

Ingólfsson, Ó., Frich, P., Funder, S., & Humlum, O. (1990). Paleoclimatic implications of an early Holocene glacier advance on Disko Island, West Greenland. *Boreas*, *19*(4), 297–311.

Kelley, S. E., Briner, J. P., & O'Hara, S. L. (2018). Assessing ice margin fluctuations on differing timescales: Chronological constraints from Sermeq Kujatdleq and Nordenskiöld Gletscher, central West Greenland. *The Holocene*, *28*(7), 1160–1172.

Kelley, S. E., Briner, J. P., & Young, N. E. (2013). Rapid ice retreat in Disko Bugt supported by ^{10}Be dating of the last recession of the western Greenland ice sheet. *Quaternary Science Reviews*, *82*, 13–22.

Kelley, S. E., Briner, J. P., Young, N. E., Babonis, G. S., & Csatho, B. (2012). Maximum late Holocene extent of the western Greenland ice sheet during the late 20th century. *Quaternary Science Reviews*, *56*, 89–98.

Kelly, M. (1973). Radiocarbon dated shell samples from Nordre Strømfjord, West Greenland: with comments on models of glacio-isostatic uplift. In *Rapport. Grønlands Geologiske Undersøgelse* (Vol. 59). Copenhagen, Denmark.

Kelly, M. (1979). Comments on the implications of new radiocarbon datesfrom the Helsteinsborg region, central West Greenland. *Rapport Grønlands Geologiske Undersøgelse*, 95, 35–42.

Kelly, M., & Funder, S. V. (1974). The pollen stratigraphy of late Quaternary lake sediments of South-West Greenland. In *Rapport. Grønlands Geologiske Undersøgelse* (pp. 1–26).

Larsen, N. K., Funder, S., Kjaer, K. H., Kjeldsen, K. K., Knudsen, M. F., & Linge, H. (2014). Rapid early Holocene ice retreat in West Greenland. *Quaternary Science Reviews*, *92*, 310–323.

Long, A. J., & Roberts, D. H. (2002). A revised chronology for the "Fjord Stade" moraine in Disko Bugt, West Greenland. *JQS. Journal of Quaternary Science*, *17*(5-6), 561–579.

Long, A. J., & Roberts, D. H. (2003). Late Weichselian deglacial history of Disko Bugt, West Greenland, and the dynamics of the Jakobshavns Isbrae ice stream. *Boreas*, *32*(1), 208–226.

Long, A. J., Roberts, D. H., & Dawson, S. (2006). Early Holocene history of the west Greenland ice sheet and the GH-8.2 event. *Quaternary Science Reviews*, *25*(9-10), 904–922.

Long, A. J., Roberts, D. H., & Wright, M. R. (1999). Isolation basin stratigraphy and Holocene relative sea-level change on Arveprinsen Ejland, Disko Bugt, West Greenland. *Journal of Quaternary Science: Published for the Quaternary Research Association*, *14*(4), 323–345.

McCarthy, D. (2011). Late Quaternary ice-ocean interactions in central West Greenland. Durham University.

Ó'Cofaigh, C., Dowdeswell, J. A., Jennings, A. E., Hogan, K. A., Kilfeather, A., Hiemstra, J. F., et al. (2013). An extensive and dynamic ice sheet on the West Greenland shelf during the last glacial cycle. *Geology*, *41*(2), 219–222. https://doi.org/10.1130/G33759.1

Philipps, W., Briner, J. P., Bennike, O., Schweinsberg, A., Beel, C., & Lifton, N. (2018). Earliest Holocene deglaciation of the central Uummannaq Fjord system, West Greenland. *Boreas*, *47*(1), 311–325.

Rinterknecht, V., Jomelli, V., Brunstein, D., Favier, V., Masson-Delmotte, V., Bourlès, D., et al. (2014). Unstable ice stream in Greenland during the Younger Dryas cold event. *Geology*, *42*(9), 759–762. https://doi.org/10.1130/G35929.1

Rinterknecht, V., Gorokhovich, Y., Schaefer, J., & Caffee, M. (2009). Preliminary ^{10}Be chronology for the last deglaciation of the western margin of the Greenland Ice Sheet. *Journal of Quaternary Science*, *24*(3), 270–278.

Roberts, D. H., Long, A. J., Schnabel, C., Davies, B. J., Xu, S., Simpson, M. J. R., & Huybrechts, P. (2009). Ice sheet extent and early deglacial history of the southwestern sector of the Greenland ice sheet. *Quaternary Science Reviews*, *28*(25-26), 2760–2773.

Roberts, D. H., Rea, B. R., Lane, T. P., Schnabel, C., & Rodés, A. (2013). New constraints on Greenland ice sheet dynamics during the last glacial cycle: Evidence from the Uummannaq ice stream system. *Journal of Geophysical Research: Earth Surface*, *118*, 519–541. https://doi.org/10.1002/jgrf.20032

Sheldon, C., Jennings, A., Andrews, J. T., Cofaigh, C. Ó., Hogan, K., Dowdeswell, J. A., & Seidenkrantz, M.-S. (2016). Ice stream retreat following the LGM and onset of the west Greenland current in Uummannaq Trough, west Greenland. *Quaternary Science Reviews*, *147*, 27–46.

Símonarson, L. A. (1981). Upper Pleistocene and Holocene marine deposits and faunas on the north coast of Nugssuaq, West Greenland. *Bulletin of Gronland Geologiske Undersogelse*, *140*, 1–9.

Storms, J. E., de Winter, I. L., Overeem, I., Drijkoningen, G. G., & Lykke-Andersen, H. (2012). The Holocene sedimentary history of the Kangerlussuaq Fjord-valley fill, West Greenland. *Quaternary Science Reviews*, *35*, 29–50.

Sugden, D. (1972). Deglaciation and isostasy in the Sukkertoppen ice cap area, West Greenland. *Arctic and Alpine Research*, 97–117.

Tauber, H. (1968). Copenhagen radiocarbon dates IX. *Radiocarbon*, *10*(2), 295–327.

Ten Brink, N. W., & Weidick, A. (1974). Greenland ice sheet history since the last glaciation. *Quaternary Research*, *4*(4), 429–440.

van Tatenhove, F. G., van der Meer, J. J., & Koster, E. A. (1996). Implications for deglaciation chronology from new AMS age determinations in central West Greenland. *Quaternary Research*, *45*(3), 245–253.

Weidick, A. (1968). *Observations on some Holocene glacier fluctuations in West Greenland*, (Vol. 165). Copenhagen, Denmark: Nyt Nordisk Forlag.

Weidick, A. (1972a). C^{14} dating of survey material performed in 1971. *Rapport. Grønlands Geologiske Undersøgelse*, *45*, 58–67.

Weidick, A. (1972b). *Notes on Holocene glacial events in Greenland*. Hofbogtrykkeri: Fr. Bagges Kgl.

Weidick, A. (1976). C^{14} dating of Survey material carried out in 1975. *Rapport. Grønlands Geologiske Undersøgelse*, *80*, 136–144.

Weidick, A. (1977). C^{14} dating of survey material carried out in 1976. *Rapport. Grønlands Geologiske Undersøgelse*, *85*, 127–129.

Weidick, A., & Bennike, O. (2007). Quaternary glaciation history and glaciology of Jakobshavn Isbrae and the Disko Bugt region, West Greenland: A review. *Geological Survey of Denmark and Greenland Bulletin*, *14*, 7–80.

Weidick, A., Bennike, O., Citterio, M., & Norgaard-Pedersen, N. (2012). Neoglacial and historical glacier changes around Kangersuneq fjord in southern West Greenland. *Geological Survey of Denmark and Greenland Bulletin*, *27*, 61.

Weidick, A., Oerter, H., Reeh, N., Thomsen, H. H., & Thorning, L. (1990). The recession of the Inland Ice margin during the Holocene climatic optimum in the Jakobshavn Isfjord area of West Greenland. *Global and Planetary Change*, *2*(3-4), 389–399.

Williams, K. M. (1993). Ice sheet and ocean interactions, margin of the east Greenland ice sheet (14 ka to present): Diatom evidence. *Paleoceanography*, *8*(1), 69–83.